

**Inclusive π^- production with 200 MeV protons:
Radiochemical study of the $^{209}\text{Bi}(p, \pi^- xn)^{210-x}\text{At}$ reactions**

J. L. Clark,* P. E. Haustein, T. J. Ruth,[†] and J. Hudis

Chemistry Department, Brookhaven National Laboratory, Upton, New York 11973

A. A. Caretto, Jr.

Department of Chemistry, Carnegie-Mellon University, Pittsburgh, Pennsylvania 15213

(Received 1 February 1982)

The results of a radiochemical study of the $^{209}\text{Bi}(p, \pi^- xn)^{210-x}\text{At}$ reactions for $x=0$ to 5 are reported. 200 MeV protons were utilized in an investigation of these pion production reactions as well as secondary processes such as $^{209}\text{Bi}(p, ^3\text{He})X$ followed by $^{209}\text{Bi}(^3\text{He}, xn)^{213-x}\text{At}$. The relative importance of such secondary reactions was deduced through variation of the target thickness and from a survey of available data from on-line investigations of ^3He production by other medium energy proton-induced reactions on ^{209}Bi . An inclusive cross section of $48 \pm 13 \mu\text{b}$ is determined for the $^{209}\text{Bi}(p, \pi^- xn)^{210-x}\text{At}$ reactions at 200 MeV. The relative yields of such $(p, \pi^- xn)$ products are found to be suggestive of a pion production mechanism involving π^- emission through coherent interactions with the target nucleons.

<p>NUCLEAR REACTIONS $^{209}\text{Bi}(p, \pi^- xn)^{210-x}\text{At}$, $E_p=200$ MeV; $^{209}\text{Bi}(p, ^3\text{He})X$, $^{209}\text{Bi}(^3\text{He}, xn)^{213-x}\text{At}$; measured σ, deduced secondary contributions and inclusive π^- production cross section; alpha particle and γ-ray spectroscopy; Si and Ge(Li) detectors, high purity targets, carrier-free radiochemistry.</p>
--

I. INTRODUCTION

Studies of nuclear reactions for which large momentum mismatches between target and projectile occur are currently being pursued at facilities such as Orsay, Saclay, TRIUMF, LAMPF, and the IUCF. Quite representative of such reactions and perhaps the one most completely studied to date is the process of pion production in proton-nucleus interactions. Such processes are of great interest to experimentalists and theoreticians alike since they are expected to provide data for the evaluation of, among other things, the high momentum components of nuclear wave functions and certain details of nuclear structure.

The results of such experimental and theoretical endeavors have been reviewed recently by Measday and Miller,¹ Höistad,² and Dillig.³ Two very general conclusions can be drawn from consideration of such papers: (1) Owing to the large momentum mismatch which characterizes the pion-production reactions, the cross sections for such processes are expected to be quite small—on the nanobarn level for single-state population in the final nucleus. (2) No single theoretical approach has been successful

in the conclusive interpretation of the available experimental results.

As a consequence of the small cross sections for pion-production reactions, the experiments typically designed to study such processes are very difficult ones. The desire to deduce the finer points of the reaction mechanism, through spectrometer measurements of angular distributions of the outgoing pions, further accentuates this problem. Despite such difficulties, recent near-threshold studies of the (p, π^+) reaction on light to medium mass nuclei have been numerous.⁴ Studies of pion production from heavier nuclei, $A \gtrsim 50$, however, have been limited due to the difficulties in resolving the particular final states populated by such reactions.

As a consequence of its “double-charge exchange” character, the (p, π^-) class of meson-production reactions has become particularly desirable to study. Although the possibility of utilizing such reactions in the pursuit of nuclear structure information seems very attractive, the fact that the cross sections for these reactions to discrete final states are typically an order of magnitude smaller than the corresponding (p, π^+) processes is reflected in the very small number of such experiments

which actually have been carried out. Nevertheless, there do exist several reports of measurements of the inclusive π^+ and π^- production, from nuclei which span the periodic table, for incident protons with kinetic energies from 585 to 730 MeV.⁵⁻⁷ Such studies utilized on-line techniques and observed total π^- production cross sections on the order of 50 mb for a heavy nucleus such as lead. These inclusive production cross sections were also seen to increase with increasing target mass by about a factor of 2 from $A \approx 100$ to $A \approx 200$.

Such results are encouraging because they suggest that inclusive π^- production cross sections at lower, nearer-threshold proton energies ($E \approx 140$ MeV) might be measurable. In particular, the choice of a suitable target-product system and sensitive radiochemical techniques can allow one to determine production cross sections to ≈ 10 nb. Such inclusive measurements are also sensitive to cases where very low energy pions are produced—a situation which exists near the reaction threshold. Spectrometer techniques, on the other hand, experience increasing difficulties when trying to detect such low-energy pions emitted from heavy nuclei.

The experiments described in this paper have measured the inclusive π^- production cross section on Bi at an incident proton energy of 200 MeV. Extensive studies of secondary reactions as well as cascade and evaporation calculations have been utilized in the correction of these radiochemically determined inclusive cross sections for such interfering effects. The results of these measurements are seen to be consistent with calculations done within the constraints of a two-nucleon model for pion production.

II. EXPERIMENTAL DETAILS

The $^{209}\text{Bi}(p, \pi^- \chi n)^{210}\text{At}$ reaction is a nearly ideal case for a radiochemical study of π^- production since such processes can be sensitively measured by appropriate activation techniques. The high sensitivity of the experiment is related to the decay characteristics of the At isotopes ($Z=85$) which are produced in this reaction. In general, the odd mass At isotopes have alpha branches of 10–50% while their even mass counterparts usually decay by electron capture. Since the electron capture daughters of such even mass species are relatively long-lived alpha emitting Po ($Z=84$) isotopes, they can be assayed with a similar level of sensitivity. The combination of high α -particle detection efficiency ($\approx 2\pi$) with near zero back-

ground and the availability of proton beam currents of the order of $1 \mu\text{A}$, permit radiochemical measurements of astatine production in bismuth targets of the order of 1 mg/cm^2 to be made for cross sections as small as a few nanobarns. The decay properties of the At and Po isotopes observed in the present investigation are summarized in Table I. It should be noted that some discrepancies between the literature values for the α decay branches of ^{207}At , ^{208}At , and ^{209}At and those measured in this study were observed. The numbers from this work were determined by comparison of the alpha decay rates of a given At source to its γ activity. Literature information concerning the γ -ray branching ratios is much more complete^{8,9} than that dealing with the α decay^{10,11} and was therefore used to calculate the α branches. Such a determination is limited by the counting rate of the γ signals as well as the relative uncertainties in the α and γ detection efficiencies. Despite these uncertainties which are approximately 7%, it is believed that these “derived” alpha branching ratios are more accurate than those currently available; and they have been utilized in all cross-section calculations presented in this paper.

The 200-MeV proton experiments were performed at the Brookhaven National Laboratory Chemistry LINAC Irradiation Facility (CLIF).¹² Proton beam currents ranging from $1 \mu\text{A}$ to $\approx 10 \mu\text{A}$ were utilized in short (10 sec to 20 min) bombardments of bismuth metal targets varying in thickness from 2 mg/cm^2 to $\approx 3 \text{ g/cm}^2$. The beam flux determinations were done by studying the production of 15.02 h ^{24}Na and 109.8 min ^{18}F in 6.8 mg/cm^2 aluminum monitor foils which were included in the bismuth target stack. Such activities are produced by the $^{27}\text{Al}(p, 3pn)^{24}\text{Na}$ or $^{27}\text{Al}(p, X)^{18}\text{F}$ reactions, the excitation functions of which are available in the literature.¹³ The use of ^{18}F activity as a flux monitor is particularly helpful in the thicker target irradiations as it is expected to be less sensitive to interfering secondary reactions which might lead to a systematic overestimation of the beam intensity. Such possible secondary processes were further checked by monitoring the proton beam flux both upstream and downstream of the target.

The bismuth targets used in the proton irradiations were prepared by one of two techniques. Thin targets ($\approx 2 \text{ mg/cm}^2$ to $\approx 35 \text{ mg/cm}^2$) were made by the evaporation of high purity bismuth metal onto aluminum backings, while thicker self-supporting targets ($\approx 1 \text{ g/cm}^2$) were prepared by

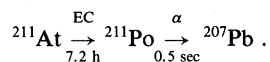
TABLE I. Decay characteristics of astatine and polonium isotopes.^a

Nuclide	$t_{1/2}$	E_α (MeV)	% α^b	E_γ (keV)	% γ
²¹¹ At	7.21 h	5.866	41.9	669.6 687.0	0.0034 0.245
²¹¹ Po ^c	0.52 sec	7.450	98.9	569.6	0.534
²¹⁰ At	8.3 h	5.131–5.524	very small	245.3 1181.4	79.4 99.3
²¹⁰ Po	138.38 d	5.304	100		
²⁰⁹ At	5.42 h	5.647	4.1(8.4)	545.0 781.9 790.2	94.4 86.6 66.0
²⁰⁹ Po	102 yr	4.882	99.7	several	all small
²⁰⁸ At	1.63 h	5.641	0.55 (2.5)	177 660 685	46.0 90.0 97.9
²⁰⁸ Po	2.898 yr	5.116	99 +	several	all small
²⁰⁷ At	1.80 h	5.759	~10 (11.5)	300.7 588.4 814.5	14 22 49
²⁰⁷ Po	5.7 h	5.116	0.008	992.3	59
²⁰⁶ At	31.4 min	5.703	0.96	395.5 477.1 700.7	48 86 97
²⁰⁶ Po	8.83 d	5.224	5.45	many	all small
²⁰⁵ At	26.2 min	5.903	10	719.3	28

^aAll information taken from Ref. 27 unless otherwise noted.

^bValues in parenthesis are from this work.

^cObserved by



subjecting a suitable quantity of bismuth metal powder to a pressure of 500 bars. Inconsistencies of target uniformity, due to the preparation technique employed, were evaluated in all cases and were found to be as large as $\pm 1\%$ for the thinnest targets studied.

Following the proton irradiations, astatine was chemically separated, in carrier-free form, from the bismuth targets. The yield for this procedure was determined through the addition of a known quantity of ²¹¹At produced by the ²⁰⁹Bi(⁴He,2n)²¹¹At reaction, to the target solution followed by an assay of ²¹¹At present after the chemical separation. Details of these radiochemical procedures have been presented elsewhere.¹⁴

Following the chemical separation, At production cross sections were determined through the use of α and γ spectroscopic techniques. Detector efficiencies for the γ -ray counting were measured by cross calibration of ²²⁸Th sources with a high resolution

Ge(Li) detector of known efficiency. Observed γ detection efficiencies for typical At γ rays varied from about 2% for $E_\gamma = 1181$ keV to about 15% for $E_\gamma = 177$ keV. Corrections due to random and true coincidence summing effects were evaluated and found to be as large as 5% for some cases involving high geometry counting. The α detector efficiency was determined by absolute calibration of $\approx 1-5$ μCi ²¹¹At sources through the measurement, by Ge(Li) counting, of the low-level 687 keV γ ray of ²¹¹At followed by α assay of the same source. Typical α detection efficiencies were on the order of 30% and were determined to approximately $\pm 5\%$. Surface barrier detectors were utilized for the α counting studies and a typical resolution for the 5.866 MeV α of ²¹¹At was about 20–30 keV FWHM.

A γ spectrum representative of the ones observed in the present investigation is illustrated in Fig. 1. With the exception of some lines assigned to iodine

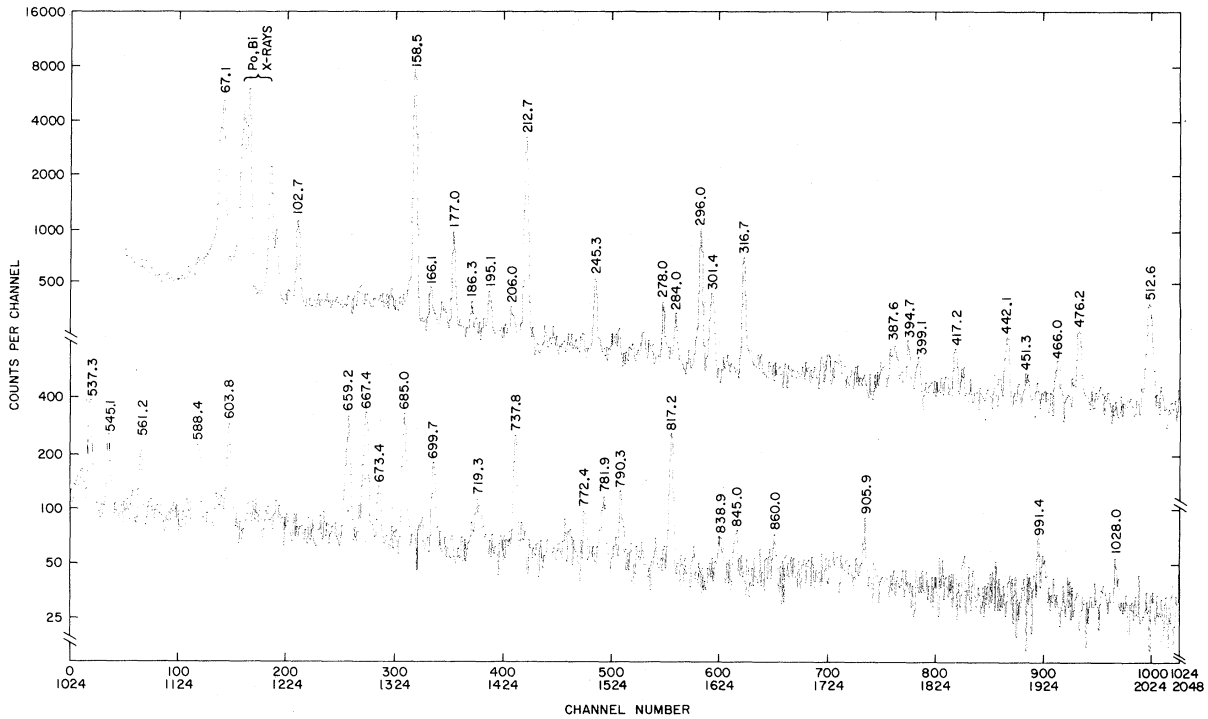


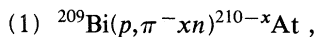
FIG. 1. Gamma-ray spectrum of a radiochemically isolated astatine source. All energies are labeled in keV. Trace quantities of gamma emitting isotopes of iodine (evidenced by the lines at 158.5, 212.7, 387.6, 442.1, 537.3, and 603.8 keV) are due to the fission of bismuth by 200 MeV protons.

isotopes produced in bismuth fission, the spectrum is dominated by the more intense gamma rays of $^{210-206}\text{At}$. Typical γ counting rates varied from $\approx 10-100$ cpm and were large enough to permit a decay curve analysis, by the CLSQ fitting routine,¹⁵ to be performed following each irradiation. Spectral peak areas were usually determined by the Brookhaven INTRAL program.¹⁶ Examples of representative alpha spectra are illustrated in Figs. 2(a) and 2(b). Hand integration techniques were used in the evaluation of α signal intensities since peak shapes and resolution were seen to vary somewhat from experiment to experiment. Total uncertainties in the disintegration rates at the end of

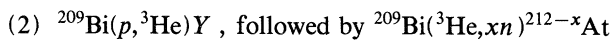
bombardment as determined by these techniques are estimated at less than 3%.

III. SECONDARY REACTIONS

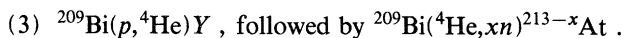
The inclusive cross sections measured by the present radiochemical technique include three major processes, the relative contributions of which must be determined in order to obtain the desired $(p, \pi^- xn)$ cross sections. The three processes which can transform the target nucleus bismuth with $Z=83$ to the product astatine with $Z=85$ are the primary reactions



as well as two secondary pathways,



and



In addition to these important processes, there exist much less likely indirect secondary reactions such as

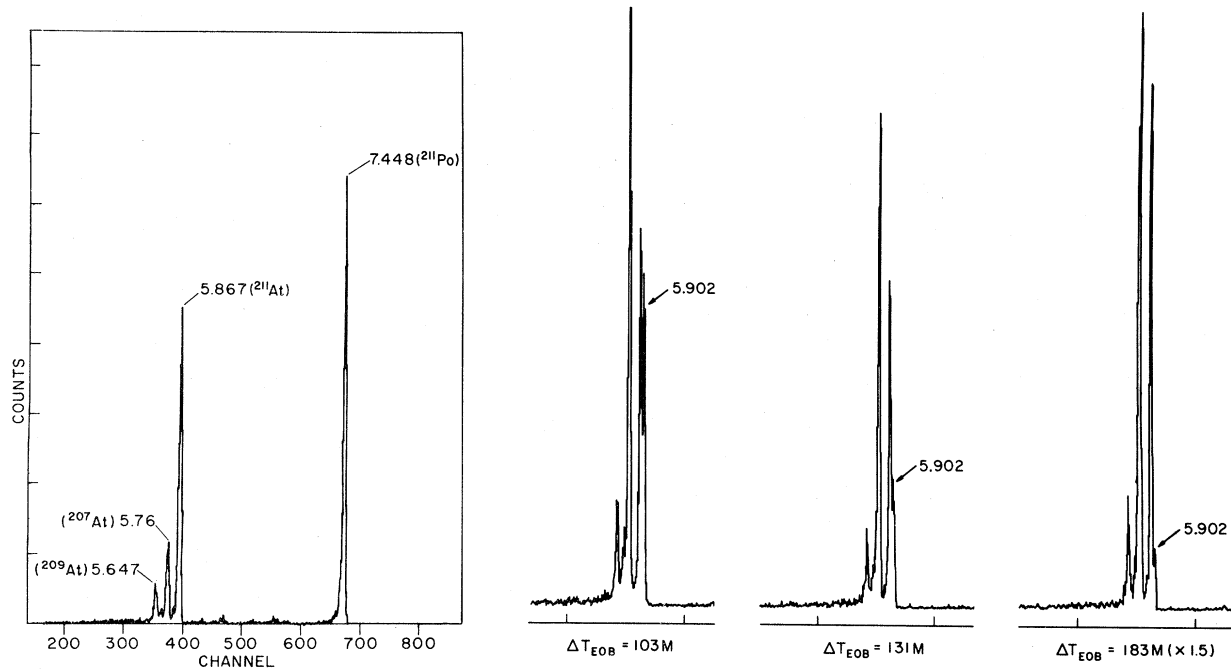
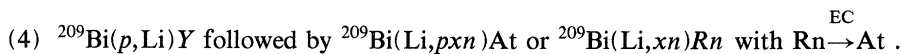


FIG. 2. Astatine alpha spectra. Part (a), the left portion of the figure, is a spectrum covering the energy region studied in the present 200-MeV proton reaction studies. Part (b), on the right, is included to demonstrate the resolution of the 26-min ^{205}At activity due to the $(p, \pi^- 5n)$ reaction from the 7.21-h ^{211}At activity due to the secondary $(^4\text{He}, 2n)$ process, at different times following the end of bombardment.



It is necessary, therefore, to evaluate the relative importance of such secondary contributions to properly interpret the results of the present experiments. The importance of complex particle-induced secondary reactions in medium energy proton bombardments of heavy nuclei has been previously discussed in detail¹⁴ and leads to the conclusion that π^- production reactions such as $^{209}\text{Bi}(p, \pi^- xn)^{210-x}\text{At}$ where $x > 2$ are essentially free of contributions from ^3He and ^4He induced secondary reactions. However, the situation applicable to the study of the more "elastic" π^- production reactions, e.g., $^{209}\text{Bi}(p, \pi^-)^{210}\text{At}$ is not so clear since secondary $^{209}\text{Bi}(^4\text{He}, 3n)^{210}\text{At}$ processes are expected to contribute as much as 1–10 μb to the inclusive ^{210}At formation cross sections measured for thick (100 mg/cm^2 to 1 g/cm^2) bismuth targets.

Since usable proton beam currents at the Brookhaven LINAC can be as high as 100 μA , a study of the target thickness dependence of the combined primary $^{209}\text{Bi}(p, \pi^- xn)^{210-x}\text{At}$ and secondary $^{209}\text{Bi}(^3, ^4\text{He}, xn)^{213-x}\text{At}$ reactions was carried out. These experiments verified that the formation of astatine isotopes with $A \leq 208$ does not occur by secondary processes, but rather takes place

by π^- production accompanied or followed by neutron emission from the intermediate At nucleus.

IV. RESULTS

Table II contains a summary of the At production cross sections measured for 200-MeV protons on Bi with chemical separation efficiencies of 100% assumed in these calculations. The cross sections for the even mass isotopes were calculated on the basis of duplicate or triplicate determinations depending on the number of different γ rays which could be detected, while the odd mass species were studied by α spectroscopy. The uncertainties quoted include, in all cases, contributions from the decay curve fitting as well as counting statistics, beam monitoring, and other sources noted earlier.

Table III presents the At production cross sections measured in the experiments in which ^{211}At spikes were added to the Bi target solutions for the determination of chemical separation efficiencies. The larger uncertainties ($\approx 25\%$) stated for these data reflect the uncertainties believed to be inherent in these chemical yield measurements. This $\pm 25\%$ value was determined in an experiment designed to

TABLE II. Relative astatine production cross sections in μb measured in the 200 MeV proton irradiations of bismuth. Isotopes marked with an * were studied by α counting; all others were done by gamma-ray spectroscopy.

Run	Bi thickness	211*	210	209*	208	207*	206	205*
309U	2.0 mg/cm ²	1.16±0.08	1.34±0.09	2.9±0.2	5.8±0.4	12.7±0.9	11.7±0.8	12.0±0.9
275	4.46 mg/cm ²	2.2 ±0.1	1.42±0.09	2.0±0.1	4.8±0.3	9.8±0.6	9.0±0.6	8.4±0.5
271	32.77 mg/cm ²	3.2 ±0.2	2.0 ±0.1	2.2±0.1	4.6±0.3	10.1±0.6	7.8±0.5	7.9±0.5
273	32.93 mg/cm ²	2.2 ±0.1	1.7 ±0.1	1.6±0.1	3.5±0.2	7.4±0.5	7.5±0.5	
258	0.71 g/cm ²	4.7 ±0.4	3.4 ±0.3	2.8±0.2	4.4±0.4	8.7±0.9	7.6±0.6	
266	0.78 g/cm ²	2.8 ±0.3	1.5 ±0.2	1.3±0.1	2.1±0.3	4.5±0.5	4.0±0.4	< 5
286	2.48 g/cm ²	3.0 ±0.2	2.0 ±0.1	1.6±0.1	2.1±0.1	4.6±0.3	3.3±0.2	
265	2.54 g/cm ²	2.8 ±0.2	1.8 ±0.2	1.4±0.1	2.4±0.3	4.3±0.4	3.5±0.3	
282	3.0 g/cm ²	2.3 ±0.2	1.7 ±0.1	1.3±0.1	1.8±0.1	3.7±0.3	2.7±0.2	

study the oxidation state mixing of At in solution.¹⁷ These At production cross sections have also been plotted in Fig. 3.

V. DISCUSSION

The first indication that two different reaction mechanisms are at play in the production of At appears in Fig. 3. Despite the rather large uncertainties of these measurements, the heavier isotopes of astatine exhibit a significant trend of decreasing cross section with decreasing target thickness. If the production of these isotopes occurs by secondary reactions, e.g., $^{209}\text{Bi}(^3,^4\text{He},xn)^{213-x}\text{At}$ for $x=2-3$, such a trend would be expected. Cross sections for isotopes of mass 205–209 do not show a similar target thickness dependence, suggesting rather strongly that a primary reaction is being observed.

Existing measurements of energy and angular distributions^{18,19} of the secondary ^3He and ^4He particles produced in medium energy proton irradiations of heavy nuclei when combined with the known excitation functions²⁰ for reactions such as $^{209}\text{Bi}(^4\text{He},xn)^{213-x}\text{At}$, provide a means of estimating secondary effects.¹⁴ Figure 4 presents the results of these calculations. Even though these esti-

mates should be applicable only to “infinitely” thick bismuth targets, there is good, qualitative agreement between the heavy At isotope cross sections predicted and those observed. The calculated trends in Fig. 4 directly reflect that the most probable secondary ^4He particle kinetic energy in these heavy target systems is about 24 MeV, and that for energies greater than this the probability of production decreases quite dramatically. It is particularly important to note that ^{211}At cannot be produced by π^- production reactions and therefore serves as an “internal monitor” of secondary ^4He particles having kinetic energies between 20 and 25 MeV. Although rather precise information about the dE/dx for ^4He particles in bismuth as well as a complete picture of the secondary-production process is needed to confidently predict cross sections for such reactions, it is apparent that the production of the lighter astatine isotopes ($A < 208$) will be suppressed relative to the production of ^{211}At since the formation of these lighter species requires secondary ^4He particle energies as high as 100 MeV. The energy requirements for secondary reactions such as $^{209}\text{Bi}(^4\text{He},xn)^{213-x}\text{At}$ and $^{209}\text{Bi}(^3\text{He},xn)^{212-x}\text{At}$ are illustrated in Fig. 5. Although the thresholds for the $(^3\text{He},xn)$ reactions are typically 15 MeV lower than the corresponding $(^4\text{He},xn)$ processes, the

TABLE III. Measured astatine production cross sections as a function of target thickness. The 3.22 g/cm² numbers are averages from duplicate determinations.

Bi target thickness	Astatine production cross section (μb)						
	211	210	209	208	207	206	205
3.22 g/cm ²	5.8±0.1	5.2±0.1	3.9±0.1	5.9±0.3	11±2	8±2	
32.77 mg/cm ²	3.8±0.9	2.4±0.6	3.0±0.8	7.4±1.8	14±3	13±3	9±2
2.0 mg/cm ²	1.5±0.4	1.8±0.4	3.7±1.0	8 ±2	17±4	15±4	16±4

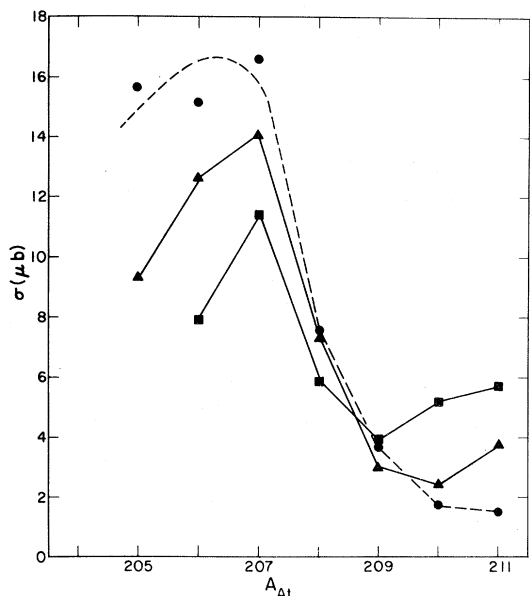


FIG. 3. Astatine production cross sections for the combined $^{209}\text{Bi}(\text{He}, xn)^{213-x}\text{At}$ and $^{209}\text{Bi}(p, \pi^- xn)^{210-x}\text{At}$ reactions. Results are from 200 MeV proton irradiations of a 2.0 mg/cm² Bi target (●), a 32.77 mg/cm² Bi target (▲), and a 3.2 g/cm² Bi target (■). All cross sections were determined through the spike addition technique and are subject to a $\pm 25\%$ uncertainty. The lines have been included to guide the eye.

number of available ^3He ions is about an order of magnitude smaller than the number of alpha particles.^{18,19} This suggests that ^3He secondary reactions make appreciable contributions only in the production of astatine isotopes with mass less than 209 (see Fig. 4). The ranges of α particles in bismuth vary from about 200 mg/cm² to 1 g/cm² for alpha energies of 25 MeV to about 100 MeV.²¹ Thus the thinner targets ($\approx 2-33$ mg/cm²) are not expected to be very sensitive to such secondary helium reactions. To check this hypothesis empirically, an irradiation of a 6.8 mg/cm² bismuth target with 135 MeV protons was carried out at the Indiana University Cyclotron Facility. At this low-beam energy, below the absolute pion production threshold, isotopes of astatine can only be made through secondary ^4He or ^3He induced reactions. This study showed that the formation of At isotopes with $A < 208$ was greatly suppressed relative to the production of ^{211}At . At isotopes with $A < 207$ were in fact not detectable at the ≈ 50 -nb cross-section sensitivity limits of this measurement.²²

These results (Fig. 3) confirm that the astatine isotopes with $A = 205-208$ are produced primarily by the $^{209}\text{Bi}(p, \pi^- xn)^{210-x}\text{At}$ reactions. Since the

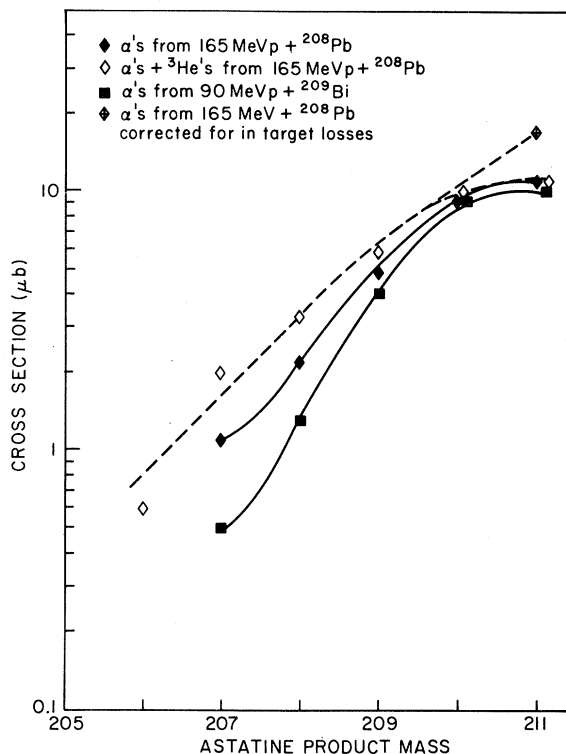


FIG. 4. Calculated astatine isotope yields for medium energy proton irradiations of very thick bismuth and lead targets. Predictions are based on the measurements of Ref. 18 (■) and Ref. 19 (◆, ◇, ◇). The in-target loss correction is based on the shorter effective range of helium ions capable of producing ^{211}At relative to the lighter astatine isotopes.

cross sections for the production of these isotopes (Table III) suffer from uncertainties of the order of 25%, an alternative approach was chosen to distinguish more clearly the competing primary and secondary processes which are at play. Plots of ratios of At cross sections as a function of Bi target thickness are shown in Figs. 6(a) and (b). The data used in these ratio calculations are taken directly from Table II. Since the determination of absolute yields is not necessary in this approach, the uncertainties due to the chemical separation procedures do not enter into such ratios. The choice of the ^{207}At cross section as a point of normalization was made since the production of ^{207}At is believed to result solely from the $^{209}\text{Bi}(p, \pi^- 3n)^{207}\text{At}$ reaction. Therefore, the ratio of the yield of any given At isotope to ^{207}At should exhibit a decrease with decreasing target thickness if secondary reactions provide the dominant pathways. On the other hand, a similar plot of the relative At isotopic yield should show

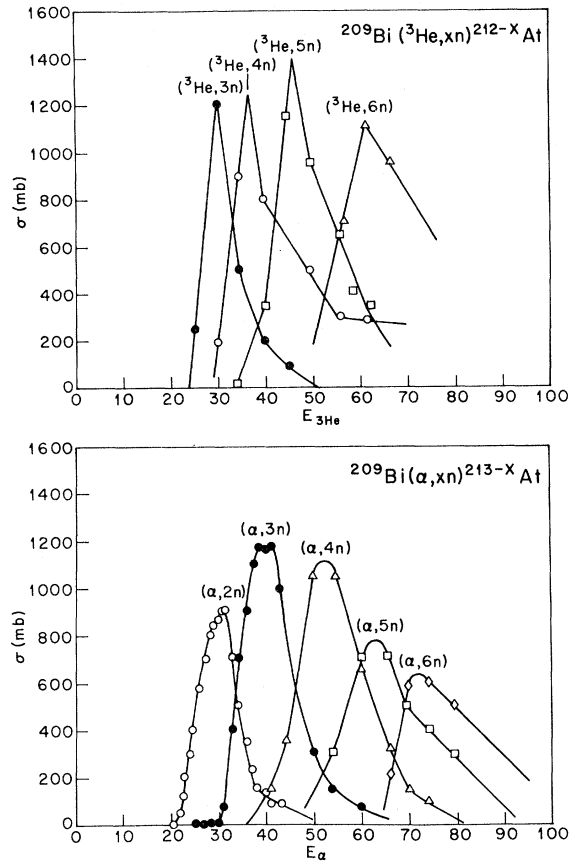


FIG. 5. Excitation functions for the $^{209}\text{Bi}(^4\text{He}, xn)^{213-x}\text{At}$ and $^{209}\text{Bi}(^3\text{He}, xn)^{212-x}\text{At}$ reactions. Data are from Ref. 20.

no target thickness dependence if π^- production reactions are the dominant ones. In Fig. 6(a), the plot of the $^{211}\text{At}/^{207}\text{At}$ yield exhibits a monotonic decrease with decreasing target thickness (T), a significant trend since it is known that the production of ^{211}At can only occur by the $^{209}\text{Bi}(^4\text{He}, 2n)^{211}\text{At}$ secondary reaction. Similar plots for the $^{210}\text{At}/^{207}\text{At}$ and $^{209}\text{At}/^{207}\text{At}$ yields show two distinct trends: firstly, an apparent decrease with decreasing thickness for targets of $\approx 3 \text{ g/cm}^2$ to $\approx 30 \text{ mg/cm}^2$ and secondly, a region ($T < 30 \text{ mg/cm}^2$) where these ratios show no significant further decrease. These trends are interpreted as due to secondary reaction domination of the At production in Bi targets thicker than about 30 mg/cm^2 , with an increasingly important contribution from the (p, π^-) reaction channels for the thinner targets. Turning now to Fig. 6(b), one sees that the trends for the lighter astatine isotopes are considerably different. The yield ratios of ^{205}At , ^{206}At , and ^{208}At to ^{207}At show no significant change with Bi target thickness

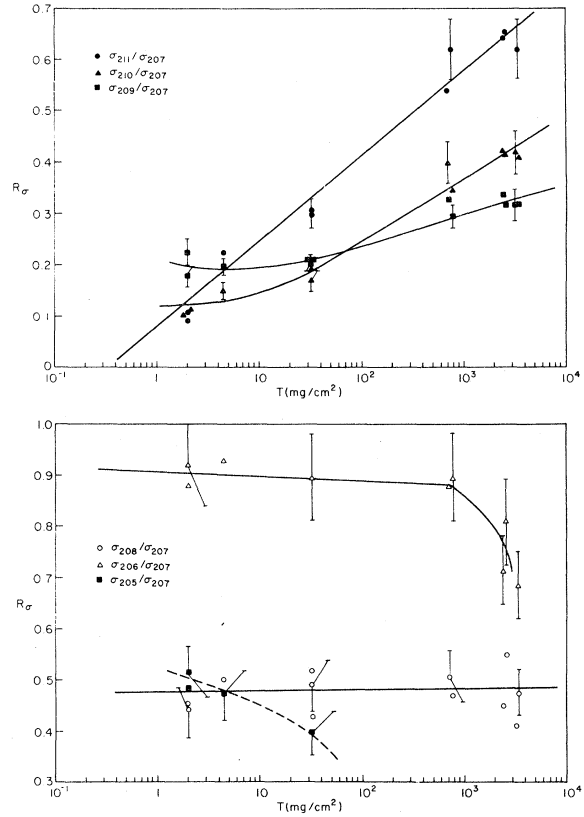


FIG. 6. Target thickness dependence of light and heavy astatine isotopes. Cross-section ratios have been calculated from the data in Table II. The lines have been drawn to guide the eye and typical error bars for a number of representative points have been shown. Note that the 205/207 numbers have been multiplied by a factor of $\frac{1}{2}$.

over most of the cases studied. If the production of the mass 205–208 astatine isotopes were dominated by the π^- production processes, with negligible contributions from secondary pathways, this would be expected.

It is difficult to interpret the trends observed for

TABLE IV. Q values for the $^{209}\text{Bi}(p, \pi^- xn)^{210-x}\text{At}$ reactions with $x = 0-6$.

Reaction	Q (MeV)
$^{209}\text{Bi}(p, \pi^-)^{210}\text{At}$	-139.0
$^{209}\text{Bi}(p, \pi^- n)^{209}\text{At}$	-146.3
$^{209}\text{Bi}(p, \pi^- 2n)^{208}\text{At}$	-154.5
$^{209}\text{Bi}(p, \pi^- 3n)^{207}\text{At}$	-162.0
$^{209}\text{Bi}(p, \pi^- 4n)^{206}\text{At}$	-170.6
$^{209}\text{Bi}(p, \pi^- 5n)^{205}\text{At}$	-178.5
$^{209}\text{Bi}(p, \pi^- 6n)^{204}\text{At}$	-187.6

the $^{206}\text{At}/^{207}\text{At}$ and $^{205}\text{At}/^{207}\text{At}$ ratios in the 1–3 g/cm² and 10–30 mg/cm² target thickness regions, respectively. Table IV presents Q values for the appropriate π^- production reactions as calculated from the 1977 mass tabulations of Wapstra and Bos.²³ The absence of the $^{209}\text{Bi}(p,\pi^-6n)^{204}\text{At}$ reaction with 200 MeV incident protons is consistent with the high Q value for this process. Energy thresholds related to the Q values for ^{205}At and ^{206}At production provide an explanation for the trends of decreasing cross section with increasing target thickness seen in Fig. 6(b). Stopping-power data²¹ indicate that 200 MeV protons will be degraded by as much as 10–15 MeV when passing through 1–3 g/cm² of Bi. Such an energy loss is consistent with the observed trends for (p,π^-xn) processes when $x > 5$.

The plots of At cross-section ratios show that most secondary reaction contributions are nearly negligible for the formation of At in Bi targets having thicknesses less than a few mg/cm². Table V summarizes the $^{209}\text{Bi}(p,\pi^-xn)^{210-x}\text{At}$ cross sections believed to be the best ones available from this analysis. Since the cross-section ratio trends in Fig. 6(b) show no indication of significant secondary contributions to the $^{205-208}\text{At}$ production at any of the target thicknesses studied, values listed for the $^{209}\text{Bi}(p,\pi^-xn)^{210-x}\text{At}$ cross sections for $x=2-5$ are taken directly from the 32.77 mg/cm² Bi target results, as these represent the target thickness region most completely investigated in these experiments.

The $^{209}\text{Bi}(p,\pi^-n)^{209}\text{At}$ cross section at 200 MeV, on the other hand, is determined by noting that the Q -value restrictions which suppress the thick target (p,π^-xn) reaction for $x=4-5$ do not apply, therefore, one can approximate the (p,π^-n) cross section at all target thicknesses by extrapolation of the 209/207 ratio data in Fig. 6(a) from the thin to thick target region. Once this is done, it is seen that secondary contributions are negligible for target thicknesses ≤ 30 mg/cm². The cross section quoted

TABLE V. Cross sections for the $^{209}\text{Bi}(p,\pi^-xn)^{210-x}\text{At}$ pion production reactions at 200 MeV.

Reaction	σ (μb)
$^{209}\text{Bi}(p,\pi^-)^{210}\text{At}$	< 1.4
$^{209}\text{Bi}(p,\pi^-n)^{209}\text{At}$	3.0 ± 0.8
$^{209}\text{Bi}(p,\pi^-2n)^{208}\text{At}$	7.4 ± 1.8
$^{209}\text{Bi}(p,\pi^-3n)^{207}\text{At}$	14 ± 3
$^{209}\text{Bi}(p,\pi^-4n)^{206}\text{At}$	13 ± 3
$^{209}\text{Bi}(p,\pi^-5n)^{205}\text{At}$	9 ± 2

in Table V is therefore also taken directly from the 32.77 mg/cm² Bi target results.

Arriving at a realistic estimate of the $^{209}\text{Bi}(p,\pi^-)^{210}\text{At}$ cross section is a considerably more difficult task. Although, as in the case of ^{209}At , there appears a target thickness region in which the total production of ^{210}At levels off, indicating the dominance of the (p,π^-) reaction channel, the larger secondary contributions at higher target thicknesses evident in Fig. 6(a) cloud the issue. Nevertheless, an analysis similar to that described for the ^{209}At case yields a $^{209}\text{Bi}(p,\pi^-)^{210}\text{At}$ cross section of $1.0 \pm 0.4 \mu\text{b}$, where the $\pm 40\%$ uncertainty is believed to be a realistic estimate for this procedure and reflects the larger contributions of the secondary processes. Owing, however, to the obvious need for additional thinner target data for ^{210}At production and the therefore tenuous nature of such an analysis in the present case, only an upper limit of $1.4 \mu\text{b}$ for the $^{209}\text{Bi}(p,\pi^-)^{210}\text{At}$ reaction based on the 2.0 mg/cm² Bi target measurement has been included in Table V.

Summing the cross sections of Table V yields a total π^- production cross section from Bi at 200 MeV of $48 \pm 13 \mu\text{b}$. The question which must be addressed at this point is whether or not this is truly an *inclusive* (p,π^-) cross section. Since the present radiochemical technique is sensitive to only π^- production processes from which $Z=85$ nuclei result, pion production channels which include charged particle emission were not investigated. However, π^- production requires at least 140 MeV of the energy of the incident proton, and thus no more than 60 MeV will be available to excite the residual nucleus following pion emission. It is also noted that the probability of competing fission processes has been assessed as negligible in these reactions. A mechanism by which the π^- is produced at rest is difficult to imagine (although not impossible); therefore, this available excitation energy will in all probability be somewhat less than 60 MeV. Calculations done with the VEGAS-DFE cascade-evaporation codes indicate that the probability of charged-particle emission from $Z=85$ nuclei excited to 50–60 MeV is only about 5–10%.²⁴ Thus, the Coulomb barrier suppression of proton and alpha particle evaporation allows one to neglect, to the $\pm 25\%$ level applicable to the present measurement, pion production channels involving charged particles.

The observation that the yield of At isotopes is considerably greater for reactions like (p,π^-xn) with $x=3-5$ than for the corresponding processes

with $x=0-2$ shows conclusively that multiple neutron emission, an energetically preferred evaporation mode for the deexcitation of heavy nuclei, is the principal mechanism by which the energy transferred to a heavy target during the pion production process is dissipated. Within the context of this proposed "model" one can estimate the kinetic energy spectrum of the negative pions (or in a similar sense, the excitation energy distribution of the residual At nuclei) produced by the 200-MeV proton reactions on Bi. Such an analysis is possible since (1) charged-particle emission does not contribute significantly at such excitation energies and (2) the highly statistical nature of the evaporation process²⁵ allows one to correlate directly the number of emitted neutrons with the average excitation energy of the residual nucleus. Here the maximum kinetic energy carried off by the pion is assumed to be approximated simply by the difference between the projectile energy in the center of mass and the Q value required by the reaction in question (see Table IV). Although an oversimplified approach, e.g., Coulomb barrier effects on pion emission, have been ignored, this analysis is expected to yield a qualitative picture of the processes at play.

The results of such an approach, involving a two-nucleon calculation done by Gibbs,²⁶ is shown (along with the present experimental numbers) in Fig. 7. This calculation allowed for the successive evaporation of neutrons from the excited ^{210}At nuclei. The ^{210}At spectrum was divided into two

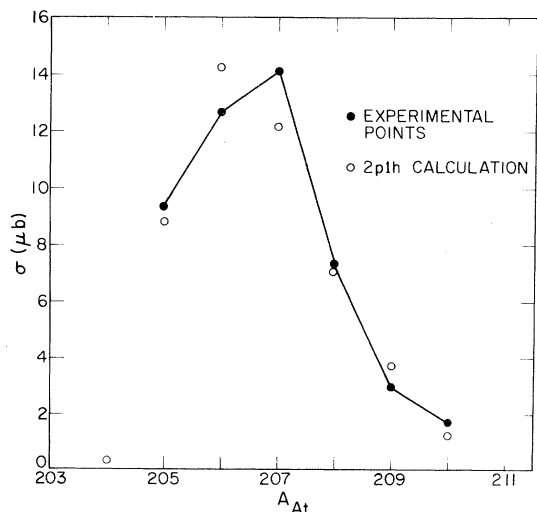


FIG. 7. The results of the Gibbs 2p-1h two-nucleon calculation (O) compared to the $(p, \pi^- xn)$ cross sections presented in Table V (●). The curve has been drawn to guide the eye.

parts: that consisting of nuclei with excitation energies less than the neutron emission threshold ($E^* < 8.3$ MeV), the integral of which is the cross section for the production of ^{210}At , and the part including nuclei having excitation energies above the neutron-emission threshold. Such excited nuclei were allowed to evaporate one neutron to lead to an excitation function for the next lighter astatine isotope. After the spectrum for ^{209}At was obtained the process was repeated to get that for ^{208}At , etc. There is good agreement between the experimental and calculated results with the cross sections for the lighter astatine isotopes demonstrating a pronounced sensitivity to the incident proton energy.

VI. SUMMARY

Radiochemical techniques have been utilized in a study of the $^{209}\text{Bi}(p, \pi^-, xn)^{210-x}\text{At}$ reactions. The high sensitivity of these techniques coupled with an assessment of the contributions of interfering secondary reactions has allowed the determination of an inclusive π^- production cross section of $48 \pm 13 \mu\text{b}$ at 200 MeV.

The observed yields of At isotopes with $A=210-205$ indicate that neutron evaporation is the principal means by which energy deposited in a heavy target nucleus through π^- production is dissipated. This is consistent with the results of a calculation whose excellent agreement with experiment further suggests the importance of multinucleon participation in π^- production.

Despite the inherent difficulties in evaluating the importance of secondary reactions in the measurement of such small inclusive cross sections, the utilization of radiochemical techniques has furnished a means for the study of some of the gross characteristics of the near threshold (p, π^-) reaction. Further similar studies would be particularly suited to surveys of pion production reactions with other heavy nuclei ($A \geq 200$) and could well provide information which would be very difficult or impossible to obtain by other experimental techniques.

ACKNOWLEDGMENTS

The assistance of Ms. E. Ritter and Ms. E. Norton in target preparation and the chemical analyses is gratefully acknowledged. The authors thank Dr. M. Hillman and Dr. L.-C. Liu for help with the DFF and ISOBAR calculations. Our appreciation is extended to Dr. W. R. Gibbs, Dr. R. R. Silbar, Prof. M. M. Sternheim, Mr. D. G. Long, Dr. T. E.

Ward, and Prof. J. M. D'Auria for their useful comments and to Dr. S. Katcoff for his help with some of the 200-MeV proton experiments. We further thank Dr. T. E. Ward for performing the 135-MeV proton irradiation and Dr. W. R. Gibbs for furnishing us results from his two-nucleon model calculations. Our special thanks go to the staff and operating crew of the Brookhaven LINAC. One of us (J.L.C.) wishes to express his appreciation to the

Chemistry Department of the Brookhaven National Laboratory for its hospitality. This research was supported in part by the U. S. Department of Energy, Office of High Energy and Nuclear Physics (J.L.C., P.E.H., T.J.R., and J.H.) and by the National Science Foundation (A.A.C.) The work of J.L.C. was performed in partial fulfillment of the requirements for the degree of Doctor of Philosophy at Carnegie-Mellon University.

*Present address: CNC-11/MS-824, Los Alamos National Laboratory, Los Alamos, NM 87545.

†Present address: TRIUMF, University of British Columbia, Vancouver, British Columbia V6T 2A3 Canada.

¹D. F. Measday and G. A. Miller, *Annu. Rev. Nucl. Part. Sci.* **29**, 121 (1979).

²B. Höistad, *Adv. Nucl. Phys.* **11**, 135 (1978).

³M. Dillig, *Nucl. Phys.* **A335**, 407 (1980).

⁴Harold W. Fearing, TRIUMF Report No. TRI-80-3, 1980 (unpublished).

⁵J. F. Crawford, M. Daum, G. H. Eaton, R. Frosch, H. Hirschmann, R. Horisberger, J. W. McCulloch, E. Steiner, R. Hausammann, R. Hess, and D. Werren, *Phys. Rev. C* **22**, 1184 (1980).

⁶J. F. Crawford, M. Daum, G. H. Eaton, R. Frosch, J. Garzon, H. Hirschmann, P. -R. Kettle, J. W. McCulloch, and E. Steiner, *Helv. Phys. Acta* **53**, 497 (1980).

⁷D. R. F. Cochran, P. N. Dean, P. A. M. Gram, E. A. Knapp, E. R. Martin, D. E. Nagle, R. B. Perkins, W. J. Schlaer, H. A. Thiessen, and E. D. Theriot, *Phys. Rev. D* **6**, 3085 (1972).

⁸B. Jonson, M. Alpsten, Å. Appelqvist, and G. Astner, *Nucl. Phys.* **A177**, 81 (1971).

⁹M. Alpsten, Å. Appelqvist, and G. Astner, *Phys. Scr.* **4**, 137 (1971).

¹⁰G. W. Barton, Jr., A. Ghiorso, and I. Perlman, *Phys. Rev.* **82**, 13 (1951).

¹¹E. K. Hyde, A. Ghiorso, and G. T. Seaborg, *Phys. Rev.* **77**, 765 (1950).

¹²S. Katcoff, J. B. Cumming, J. Godel, V. J. Buchanan, H. Susskind, and C. J. Hsu, *Nucl. Instrum. Methods* **129**, 473 (1975).

¹³J. B. Cumming, *Annu. Rev. Nucl. Sci.* **13**, 261 (1963).

¹⁴J. L. Clark, P. E. Haustein, T. J. Ruth, J. Hudis, and A. A. Caretto, Jr. *Phys. Rev. C* (to be published).

¹⁵J. B. Cumming, National Academy of Sciences—National Research Council, Nuclear Science Series Report No. NAS-NS-3107, 1962 (unpublished).

¹⁶J. B. Cumming (unpublished), based on modifications of a program by R. Gunnink, H. B. Levy, and J. B. Niday, University of California Radiation Laboratory Report No. UCID-15140 (unpublished).

¹⁷J. L. Clark, thesis, Carnegie-Mellon University, 1980 (unpublished).

¹⁸J. R. Wu, C. C. Chang, and H. D. Holmgren, *Phys. Rev. C* **19**, 698 (1979).

¹⁹R. E. Segal (private communication).

²⁰J. D. Stickler and K. J. Hofstetter, *Phys. Rev. C* **9**, 1064 (1974).

²¹L. C. Northcliffe and R. F. Schilling, *Nucl. Data Tables* **A7**, 233 (1970).

²²T. E. Ward and J. L. Clark (unpublished).

²³A. H. Wapstra and K. Bos, *At. Data Nucl. Data Tables* **19**, 175 (1977).

²⁴J. L. Clark and L.-C. Liu (unpublished).

²⁵I. Dostrovsky, Z. Fraenkel, and G. Friedlander, *Phys. Rev.* **116**, 683 (1959).

²⁶W. R. Gibbs, *Pion Production and Absorption in Nuclei—1981 (Indiana University Cyclotron Facility)*, Proceedings of the Conference on Pion Production and Absorption in Nuclei, AIP Conf. Proc. No. 79, edited by Robert D. Bent (AIP, New York, 1982).

²⁷*Table of Isotopes*, 7th ed., edited by C. M. Lederer and V. S. Shirley (Wiley, New York, 1978).